Reports

Enhanced Ethylene and Ethane Production with Free-Radical Cracking Catalysts

JOHN H. KOLTS AND GARY A. DELZER

A series of free-radical catalysts have been discovered that increase the yield of highly valuable olefins from the cracking of low molecular weight paraffins. For example, catalytic cracking of *n*-butane, isobutane, and propane over manganese or iron supported on magnesium oxide (MgO) gave product distributions different from those given by thermal (free-radical) cracking or cracking over traditional acid catalysts. With *n*-butane and propane feeds, the products from catalytic cracking included large amounts of ethylene and ethane; with isobutane feed, propylene was the major product. Physical characterization of the MgO-supported catalyst showed the manganese to be in a 2+ oxidation state in the reduced catalyst and a 4+ oxidation state in the fully oxidized catalyst. Manganese was also shown to be uniformly distributed in the support material with very little enrichment at the surface. Matrix isolation of the gas-phase radicals from *n*-butane feed showed that ethyl and methyl radicals were produced over the active catalysts. In the thermal process, only methyl radicals were produced. The mechanism of the catalytic reaction appears to be selective formation of primary carbanions at the catalyst surface followed by electron transfer and release of primary hydrocarbon radicals to the gas phase.

INDUSTRIAL PRODUCTION OF LIGHT olefins from low molecular weight hydrocarbons has been dominated by noncatalytic processes in which cracking takes place simply by heating the hydrocarbons to very high temperature (*1*). These thermal processes are called free-radical cracking. Catalytic processes aimed at producing low molecular weight olefins have not been successful because of low selectivity to the desired olefin, high rates of coke formation, or excessive methane production (*2, 3*). The relatively low selectivity to a specific product in both catalytic and noncatalytic cracking can be traced directly to the nonselective activation of the feed hydrocarbon.

We have shown that manganese or iron supported on MgO gives product distributions different from those given by free-radical cracking or state-of-the-art cracking catalysts. Table 1 shows the product distributions from cracking *n*-butane with manganese and iron catalysts and from the homogeneous free-radical cracking of *n*-butane over inert fused silica. The data show the changes in product selectivities, as well as increases in conversion level, obtained with the MgO-supported catalysts. Table 2 shows comparable data for the catalytic cracking of propane and isobutane over the Mn-MgO catalyst. Experiments conducted with ethane and methane feeds did not show catalytic effects. All experiments were performed in a conventional downflow reactor constructed of fused silica (*4*). The catalysts were prepared either by impregnation of $Mg(OH)_2$ with a water-soluble manganese or iron salt or by blending finely powdered $Mg(OH)_2$ with manganese or iron nitrates dissolved in just enough water to form a thick paste. In both preparations, the dried catalysts were calcined at 800°C in air before testing. All data shown are representative of several runs. The random-error uncertainty for the measurements in the tables and figures is ±10 percent on the basis of 95 percent limits from a long-term sequence of measurements relative to gas chromatographic standards.

Adelson and Sokolovskaya (*5*) reported that a 20 percent KVO_3-pumice catalyst, compared with thermal cracking, increased conversion of *n*-butane and improved selectivity to ethylene. They suggested (*6*) that the changes in product selectivity were due to the increased concentration of all radical species rather than a fundamental change in the hydrocarbon activation mechanism. With *n*-butane feed, traditional acid cracking catalysts tend to produce increased selectivity to propylene and methane. This is intrinsic to a carbenium ion–cracking mechanism (*2, 3*). Our data do not support either a simple increase in the concentration of free radicals or a carbenium ion–based mechanism for manganese or iron on MgO.

In addition to manganese and iron supported on MgO, several other combinations of metals and supports were evaluated for the selective cracking of propane, *n*-butane, and isobutane. Cobalt and chromium were expected to behave similarly to manganese and iron; however, Cr-MgO showed only dehydrogenation activity, and Co-MgO showed high selectivity to methane and coke. Other support materials, such as La_2O_3 and CeO_2, were active catalysts when impregnated with manganese, but in no case was the activity as high as that observed over MgO. Other traditional catalyst supports, for example, Al_2O_3, SiO_2, Al_2O_3-SiO_2, TiO_2, and ZrO_2, showed no selective cracking of the feeds tested. Because of the similarities of CaO and MgO in terms of electronic structure, crystal structure, and basic properties, we expected that CaO would be an active support material; however, manganese or iron supported on CaO showed no catalytic activity within experimental error.

Measurement of catalytic activity as a function of time showed that, after passing *n*-butane over the catalyst for 30 seconds, the percent conversion and product selectivity returned to the values given by thermal cracking. Addition of steam, however, increased the active life of the catalyst. The active life of the catalyst was further improved by the addition of 2 to 7 percent calcium to the catalyst. Calcium appeared to be an effective promoter only in the presence of steam. Figure 1 shows the relative activity at several steam concentrations as a function of time. The loss of catalyst activity appeared

Table 1. Results from catalytic cracking of *n*-butane compared with those from thermal (free-radical) cracking over fused silica. Catalysts were prepared as 4% metal by weight on the MgO support. Test conditions: 17 cubic centimeters of −20/+40 mesh particles; temperature, 725°C; pressure, 1 atmosphere; feed flow, 100 cubic centimeters per minute at standard temperature and pressure; and ratio of steam to hydrocarbon, 1 to 1. Selectivities are calculated on the basis of moles of feed (carbon-based) converted to a particular product. Error limits are ±10% (see text).

Catalyst	Conversion (%)	Product selectivity (%)			
		Ethylene	Ethane	Propylene	Methane
Fused silica	35	23	9	41	19
Mn-MgO	65	43	22	21	10
Fe-MgO	68	38	17	22	15

Phillips Research Center, Phillips Petroleum Company, Bartlesville, OK 74004.

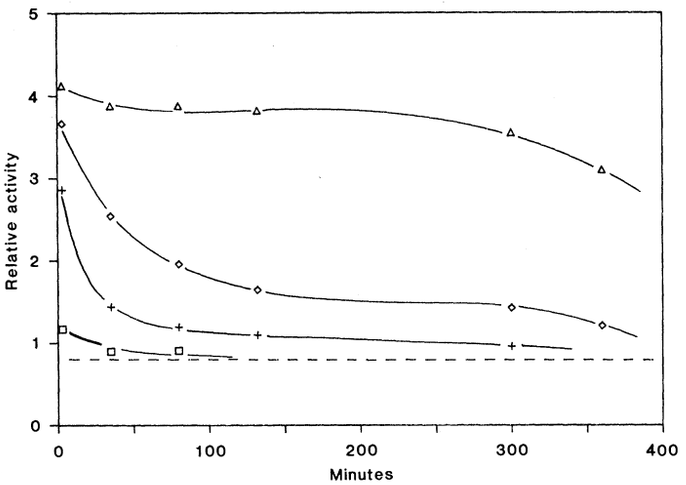

Fig. 1 (left). Effect of steam on relative activity of 4% Mn–3% Ca-MgO catalyst with *n*-butane as the feed. Reactor temperature was 725° ± 3°C. Ratio of steam to hydrocarbon: △, 2 to 1; ◇, 1 to 1; +, 0.5 to 1; □, 0 to 1. The dashed line indicates activity for noncatalytic free-radical cracking under the same conditions.

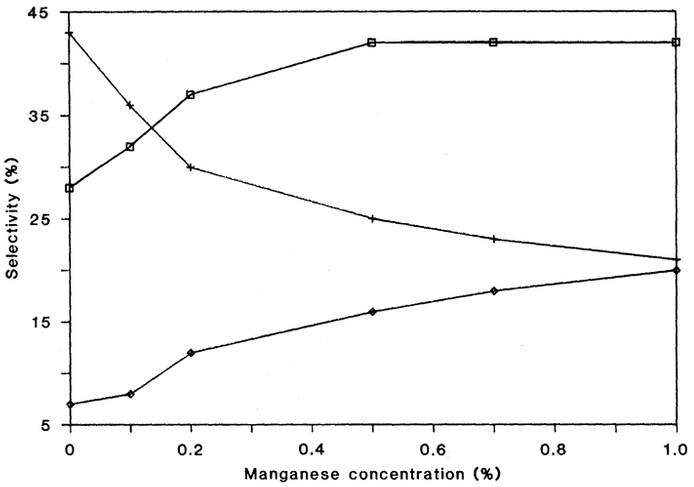

Fig. 2 (right). Product selectivities from *n*-butane as a function of manganese concentration (%) supported on MgO. Test conditions: reactor temperature, 700° ± 3°C; the ratio of steam to hydrocarbon, 1 to 1; feed flow, 100 cubic centimeters per minute at standard temperature and pressure. Samples were taken 2 minutes after feed was started. For clarity, conversion and methane selectivity are not shown; methane selectivity declined at the same rate as propylene selectivity. Selectivities: □, ethylene; ◇, ethane; +, propylene.

to be due to the deposition of coke on the active catalyst surface. Analysis of used catalysts showed that 2.3 percent coke by weight was present when the catalyst was fully deactivated. The improved catalyst life in the presence of steam was attributed to the reaction of steam and carbon to produce CO_x and hydrogen. Calcium promoter increased the rate of this reaction. Fully deactivated catalysts were restored to their initial activity by air oxidation or by extended steaming in the absence of hydrocarbon. The catalyst was cycled between hydrocarbon feed and air regeneration more than 400 times, with no degradation of activity.

The effects of manganese concentration on *n*-butane cracking are shown in Fig. 2. The addition of small amounts of manganese increased the selectivity to ethylene with maximum selectivity reached at 0.5 percent manganese. Ethane selectivity did not increase as rapidly; its maximum was reached at 1 percent manganese. The selectivities for propylene and methane decreased with the addition of manganese. Between manganese concentrations of 1 and 17 percent, the observed selectivities did not change within experimental error.

An increase in conversion from 24 to 47 percent was also observed when the manganese concentration was increased from 0 to 1 percent. The conversion increased again, to 57 percent, at a manganese concentration of 17 percent. Measurement of catalyst activity as a function of temperature and *n*-butane concentration, with a 4 percent Mn–3 percent Ca-MgO catalyst, gave an apparent activation energy of 53 kcal per mole and showed a first-order dependence on hydrocarbon concentration.

Thermal gravimetric studies in which the Mn-MgO catalyst was cycled between hydrocarbon or hydrogen reduction and air oxidation indicated there was an exchange of almost one oxygen atom per manganese atom. X-ray powder diffraction patterns showed the presence of Mg_6MnO_8 in the oxidized catalyst and MnO in the reduced catalyst. However, MnO was only detected at manganese concentrations greater than 10 percent; at lower concentrations, no manganese-containing species were detected. X-ray photoelectron spectroscopy (XPS) of oxidized and reduced samples also suggested that Mn^{4+} and Mn^{2+}, respectively, were the predominant manganese oxidation states. Similar analyses of Mn-SiO_2 and Mn-Al_2O_3 showed the oxidized form was Mn_3O_4 and the reduced form was MnO. When manganese was supported on CaO, the oxidized form was present as Ca_2MnO_4. XPS measurements on catalytically active Mn-MgO indicated that most of the manganese was uniformly distributed throughout the MgO lattice with only slight enrichment at the catalyst surface.

Matrix isolation experiments (*7*) were conducted in which radicals produced over fused silica, MgO, and Mn-MgO were frozen out of the gas phase into an argon matrix at 13 K. The radical species in the matrix were identified by electron paramagnetic resonance (EPR) spectroscopy. After *n*-butane feed was used, the EPR spectra showed that only methyl radicals were trapped from fused silica and MgO. With the Mn-MgO catalyst, approximately 35 percent of the trapped radicals were ethyl radicals, and the remainder were methyl radicals. The increase in ethyl radical concentration was even more dramatic after we had taken into account the relatively rapid unimolecular decomposition of ethyl radicals between the catalyst and collection zone.

A proposed mechanism for the controlled cracking of hydrocarbons over the supported manganese and iron catalysts is shown in Fig. 3. The active catalytic site may be

Table 2. Results from cracking propane and isobutane over 8% Mn–MgO catalyst compared with those from thermal (free-radical) cracking over fused silica. Test conditions are the same as in Table 1 except temperature: propane, 700°C; isobutane, 675°C. Selectivities are calculated on the basis of moles of feed (carbon-based) converted to a particular product. Error limits are ±10% (see text).

Catalyst	Conversion (%)	Product selectivity (%)				
		Ethylene	Ethane	Propylene	Butenes	Methane
			Propane			
Fused silica	38	36	3	40	2	19
Mn-MgO	61	46	3	21	0	28
			Isobutane			
Fused silica	32	3	1	31	50	14
Mn-MgO	59	3	1	47	23	23

isolated manganese or iron atoms stabilized in the 3+ oxidation state by the MgO lattice. Hydrocarbon could interact with the surface to form a stabilized carbanion, and then electron transfer could occur with subsequent release of a hydrocarbon free radical into the gas phase. The active catalytic site could then be regenerated by means of hydrogen atom recombination at the surface and abstraction of the surface-bound hydrogen by gas-phase radicals.

Several aspects of the proposed mechanism are critical to explaining the experimental data. Initial formation of carbanions at the surface would direct activation of the hydrocarbon to the primary position as a result of the inherent carbanion stabilities (primary > secondary > tertiary). Steric hindrance could also direct activation to the primary position; the ability of pure MgO to form carbanions at the surface has been reported (*8*). Electron transfer and subsequent desorption of hydrocarbon radicals would result in the directed formation of primary radicals. Gas-phase radical decomposition by means of accepted pathways of

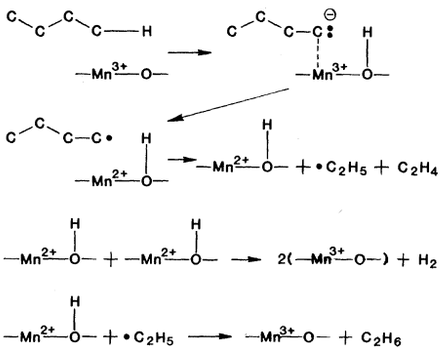

Fig. 3. Proposed mechanism for the selective cracking of *n*-butane over the Mn-MgO catalyst.

carbon-carbon bond scission would then produce the observed changes in product selectivities. The anomalously high selectivity to ethane observed during *n*-butane cracking could be attributed to abstraction of hydrogen from the catalyst surface by ethyl radicals. Alternative explanations, such as gas-phase hydrogen atom abstraction or catalytic hydrogenation of ethylene, are not likely. If most of the ethane were formed by gas-phase abstraction processes, the ratio of ethane to ethylene would be near that observed for thermal conversions under comparable reaction conditions. Experiments in which ethylene and hydrogen were passed over the Mn-MgO catalyst showed it had virtually no hydrogenation activity.

REFERENCES AND NOTES

1. W. H. Corcoran, in *Pyrolysis: Theory and Industrial Practice*, L. F. Albright, B. L. Crynes, W. H. Corcoran, Eds. (Academic Press, New York, 1983), pp. 47–68.
2. B. C. Gates, J. R. Katzer, G. C. A. Schuit, *Chemistry of Catalytic Processes* (McGraw-Hill, New York, 1979), pp. 10–45.
3. W. O. Haag and R. M. Dessau, in *Proceedings of the 8th International Congress on Catalysis*, G. Ertl, Ed. (Verlag Chemie, Weinheim, Federal Republic of Germany, 1984), vol. 2, pp. 305–316.
4. J. H. Kolts, in preparation.
5. S. V. Adelson and V. G. Sokolovskaya, *Kinet. Catal.* (Engl. Transl.) **22**, 247 (1981).
6. V. G. Sokolovskaya and S. V. Adelson, *Neftekhimiya* **24**, 371 (1984).
7. W. Martir and J. H. Lunsford, *J. Am. Chem. Soc.* **103**, 3728 (1981).
8. E. Garrone and F. S. Stone, in *Proceedings of the 8th International Congress on Catalysis*, G. Ertl, Ed. (Verlag Chemie, Weinheim, Federal Republic of Germany, 1984), vol. 3, pp. 441–452.

12 November 1985; accepted 13 March 1986

Inorganic and Organic Sulfur Cycling in Salt-Marsh Pore Waters

GEORGE W. LUTHER III,* THOMAS M. CHURCH, JOSEPH R. SCUDLARK, MONIQUE COSMAN

Sulfur species in pore waters of the Great Marsh, Delaware, were analyzed seasonally by polarographic methods. The species determined (and their concentrations in micromoles per liter) included inorganic sulfides (≤3360), polysulfides (≤326), thiosulfate (≤104), tetrathionate (≤302), organic thiols (≤2411), and organic disulfides (≤139). Anticipated were bisulfide increases with depth due to sulfate reduction and subsurface sulfate excesses and *p*H minima, the result of a seasonal redox cycle. Unanticipated was the pervasive presence of thiols (for example, glutathione), particularly during periods of biological production. Salt marshes appear to be unique among marine systems in producing high concentrations of thiols. Polysulfides, thiosulfate, and tetrathionate also exhibited seasonal subsurface maxima. These results suggest a dynamic seasonal cycling of sulfur in salt marshes involving abiological and biological reactions and dissolved and solid sulfur species. The chemosynthetic turnover of pyrite to organic sulfur is a likely pathway for this sulfur cycling. Thus, material, chemical, and energy cycles in wetlands appear to be optimally synergistic.

THE BIOGEOCHEMICAL ROLE OF SULfur in tidal wetlands is an area of intense research. Because sulfur is an important redox element under natural aquatic conditions, it is responsible for a number of important biogeochemical processes, such as sulfate reduction (*1, 2*), pyrite formation (*2, 3*), metal cycling (*4–6*), salt-marsh ecosystem energetics (*7, 8*), and atmospheric sulfur emissions (*9, 10*). Each of these processes depends upon the formation of one or more sulfur intermediates, which may have any oxidation state between +6 and −2. The intermediate oxidation states of sulfur may be organic or inorganic (*11*). For example, pyrite, FeS_2, forms readily when polysulfides (S_x^{2-}) are present (*12*). Pyrite can store reduced sulfur compounds, and its oxidation is believed to support salt-marsh food webs (*7, 8*). Once buried, pyrite appears geologically stable and is a primary reservoir of iron and sulfur in salt-marsh sediments (*2, 3*).

At present, our knowledge of the modes of formation and concentrations of organic sulfur compounds in natural aquatic systems is limited (*11*). In salt-marsh pore waters and sediments, such compounds may be precursors of organic sulfur in fossil fuels such as coal. The emission of organic sulfur compounds from tidal wetlands to the atmosphere may be an important remote source of stable, reduced sulfur compounds (*9*), which, when oxidized, act as remote acid rain precursors (*13*). The role of organic sulfur compounds in other biogeochemical processes in estuaries is not clear, although active participation in trace metal cycling appears likely (*4*).

Adequate methods for the determination of sulfur species in natural waters have only recently become available. Several species of sulfur in pore waters from Great Marsh, Delaware, were found at three depths during the summer period as a result of investigations with electrochemical titration methods and ultraviolet-visible spectroscopy (*4*);

G. W. Luther III and M. Cosman, Department of Chemistry-Physics, Kean College of New Jersey, Union, NJ 07083. T. M. Church and J. R. Scudlark, College of Marine Studies, University of Delaware, Newark, DE 19716.

*To whom correspondence should be addressed at College of Marine Studies, University of Delaware, Lewes, DE 10058.